The 225-year precipitation variability inferred from tree-ring records in Shanxi Province, the North China, and its teleconnection with Indian summer monsoon

Qiang Li, Yu Liu, Takeshi Nakatsuka, Huiming Song, Danny McCarroll, Yinke Yang, Jun Qi

PII: S0921-8181(15)00125-3
DOI: doi: 10.1016/j.gloplacha.2015.06.005
Reference: GLOBAL 2288

To appear in: *Global and Planetary Change*

Received date: 8 January 2015
Revised date: 10 June 2015
Accepted date: 21 June 2015

Please cite this article as: Li, Qiang, Liu, Yu, Nakatsuka, Takeshi, Song, Huiming, McCarroll, Danny, Yang, Yinke, Qi, Jun, The 225-year precipitation variability inferred from tree-ring records in Shanxi Province, the North China, and its teleconnection with Indian summer monsoon, *Global and Planetary Change* (2015), doi: 10.1016/j.gloplacha.2015.06.005

The 225-year precipitation variability inferred from tree-ring records in Shanxi Province, the North China, and its teleconnection with Indian summer monsoon

Authors:

Qiang Li [a,b*], Yu Liu [a,b,c*], Takeshi Nakatsuka [d], Huiming Song [a], Danny McCarroll[e], Yinke Yang[f], Jun Qi[g]

Author affiliations:

[a] State Key Laboratory of Loess and Quaternary Geology, Institute of Earth Environment, Chinese Academy of Sciences, Xi'an 710061, China

[b] Joint Center for Global Change Studies (JCGCS), Beijing 100875, China

[c] School of Human Settlements and Civil Engineering, Xi'an Jiaotong University, Xi'an 710049, China

[d] Research Institute of Humanity and Nature, 457-4 Motoyama, Kamigamo, Kita-ku, Kyoto 603-8047, Japan

[e] Department of Geography, University of Wales Swansea, Swansea, SA2 8PP, UK

[f] Environmental Science and Engineering Collage, Chang'an University, Xi'an 710054, China

[g] Nature Reserve Administration of Xinglong Mountain , Lanzhou 730100, China

Correspondence information:

*Qiang Li, *Yu Liu

TEL: +86-29-6233-6226

Fax: +86-29-6233-6234

E-mail: liqiang@ieecas.cn; liuyu@loess.llqg.ac.cn

Abstract

Understanding the interactions between the East Asian summer monsoon and Indian summer monsoon is a challenging task because of the insufficient proxy records. In this study, we reconstructed a 225-year precipitation record by combining ring widths of *Pinus tabulaeformis* and stable oxygen isotope ratios of *Larix principis-rupprechtii* using a multi-proxy dendroclimatology approach in the North China. The reconstructed record explained 51.9% of the variance in the observed precipitation during 1955-2003. The precipitation series could indicate the intensity of the East Asian summer monsoon. A spatial field analysis indicated that the series was strongly correlated with the reconstructed records of the surrounding area and a large part of the Indian subcontinent. The reconstructed records were significantly and positively correlated with All Indian Precipitation records (r=0.32, n=132, p<0.001) and with a proxy of the Indian summer monsoon. These findings suggest that a persistent teleconnection exists between the reconstructed record and the Indian summer monsoon records from the past 225 years. The observed interannual synchronisation potentially resulted from the transport of partial water vapour from the Indian Summer Monsoon area to NC; however, this synchronisation could not be attributed to the El Nino-South Oscillation (ENSO). When considering an interdecadal time scale, the synchronisation with the North Atlantic Oscillation (NAO) has varied since 1779, implying that the NAO may serve as an additional atmospheric

pattern that affects this teleconnection.

1. Introduction

The Asian Summer Monsoon system, including the East Asian summer monsoon (hereafter, EASM) and the India summer monsoon (hereafter, ISM), is important for economic development and agricultural production in dozens of countries and impacts approximately half of the world's population (Wu et al., 2012a). In the EASM area, especially in the North China (NC, between32°-42°N and 110°-120°E), meteorologists have shown that precipitation declines when the ISM is below normal (Feng and Hu, 2004; Hu et al., 2005; Huang and Wang, 2007; Liu and Ding, 2008; Zhang, 1999). However, the dynamic mechanisms of this decline are not fully understood (Wang et al., 2003), and the above results are based on a short series of meteorological measurements (typically since the 1950s in China) that were obtained during a time of rapidly changing atmospheric chemistry (Crowley, 2000; Etheridge et al., 1998), possible unprecedented warming (D'Arrigo et al., 2006; Frank et al., 2010; Mann et al., 2008) and unusual solar activity (Solanki et al., 2004). In addition, based on observational data and numerical simulation experiments, a previous study indicated that the precipitation in the EASM area is sustained by a branch of the ISM water vapour (Wu et al., 2012a). It is unknown if such water vapour transport existed before the instrumental era.

A long-term perspective is needed to interpret the stability of the proposed links

between the precipitation of NC and ISM, infer the likely mechanistic controls, and explore the implications for modelling future climate change. In the NC, a large number of tree-ring based climate reconstructions have been published in the past decades. Some temperature reconstructions (Bao et al., 2012; Ma et al., 2015) and mositure-related reconstructions (Chen et al., 2012; Fang et al., 2009; Li et al., 2007; Li et al., 2006; Liang et al., 2006; Liu et al., 2010; Shen et al., 2008; Yi et al., 2012) have been carried out. However, few comparisons of precipitation in NC and the ISM region before instrumental measurements have been published. Additionally, only a few decades of observed meteorological records are available, limiting our ability to understand the low-frequency characteristics of the long-term relationship between precipitation of NC and ISM.

In this study, we combined tree-ring widths and stable oxygen isotope ratios from two different tree species to produce an annual resolution reconstruction of the precipitation variations in Shanxi Province, NC, since AD 1779. Next, the precipitation reconstruction was compared with the ISM index using instrumental precipitation measurements that extended to 1871 in India and a longer reconstruction of the ISM index based on coral proxies. Finally, possible forcing mechanisms of the interactions at different time scales were examined by employing large-scale atmospheric circulation indexes.

2. Materials and Methods

Our sampling sites are located in the semi-arid Shanxi Province in NC. Tree rings were sampled at two sites with different hydrological conditions. The distance between the two sampling sites is only 25 km (Figure 1). The Ningwu site is located on a dry, rocky ridge (38°50′N, 112°05′E; 1600-2100 m *asl*) where 37 cores were collected from 17 Chinese pine trees (*Pinus tabulaeformis*) and carefully cross-dated to build a ring-width chronology. The detailed statistical data are shown in Table S1. The effective length, where the subsample signal strength (SSS) is at least 0.75 (Wigley et al., 1984), corresponds with the period from 1779 to 2003 because of low sample depth (Li et al., 2006), whereas the Expressed Population Signal (EPS) is higher than 0.85 since 1810. The sample size and running Rbar (mean of the correlation coefficients among the samples) are also shown in Figure S1.

The other site, Luya Mountain, is located in an alpine meadow (38°44′N, 111°50′E; 2400~2600 m *asl*). We collected samples from the dominant species of NC larch (*Larix principis-rupprechtii)* in 2004. Tree-ring width data from NC larch were previously analysed (Yi et al., 2006). Four tree-ring cores of NC larch were chosen that covered a period of 1675-2003 to measure the annual $\delta^{18}O$ values (Figure S2). Four tree-ring $\delta^{18}O$ series presented a very high correlation (r>0.90) and expressed a significant population signal (EPS>0.85) (Wigley et al., 1984) during the overlapping period. Details regarding the chemical extraction of cellulose and the construction of the tree-ring $\delta^{18}O$ series were described by Li et al. (2011a; 2011b).

Previously, preliminary studies were conducted using the tree-ring width index and the $\delta^{18}O$ data mentioned above (Li et al., 2006; 2011a). These preliminary studies aimed to reconstruct precipitation variations in Ningwu and to represent hydroclimate-sensitive $\delta^{18}O$ variations at Luya Mountain. To understand different and more issues (*e.g.*, unsolved meteorological/atmospheric hotspots), this study aimed to investigate the relationships between EASM and ISM and their associated causes in the pre-instrument era by using improved reconstructions that combined both data series (the tree-ring width and $\delta^{18}O$) from the two tree species.

McCarroll et al. (2003) proposed a 'multi-proxy dendroclimatology' approach for strengthening climate reconstructions by using different tree-ring parameters (*e.g.*, width, density and stable isotopes). In multi-proxy dendroclimatology, the dominating climatic control over different tree-ring parameters remains the same, while the secondary climatic control varies. Previous studies have demonstrated that local precipitation dominantly controls tree-ring widths in Chinese pine and $\delta^{18}O$ in NC larch, whereas relative humidity and temperature exert secondary control (Li et al., 2006; Li et al., 2011b). In this study, we use the multi-proxy dendroclimatology approach to enhance the explained variance of the precipitation reconstruction. A simple linear multi-regression was used to combine the precipitation signals from the tree-ring widths (Chinese pine) and $\delta^{18}O$ contents (NC larch).

The combined proxies were calibrated using the nearest meteorological station in Yuanping (38°45′N, 112°42′E; 836 m *asl*). The mean annual precipitation was 428

mm during the observation period (1954-2003). The highest precipitation occurred during the monsoon season (July-September) and accounted for almost 80% of the total annual precipitation. The instrumental records of the Indian precipitation from 1871 to 2003 are based on the summed All Indian Precipitation data provided by the Indian Institute of Tropical Meteorology (http://www.tropmet.res.in/), which could be as the ISM index. To facilitate this comparison, we used Indian precipitation data from the same period (previous August to current July) of our reconstruction in Section 3. Before the instrument period, we relied on a high-resolution coral-based reconstruction of the strength of the low-level cross-equatorial jet of the western Indian Ocean (Gong and Luterbacher, 2008), which is regarded as a reliable indicator of the ISM index. The spatial pattern of the correlation was plotted using KNMI Climate Explorer (http://climexp.knmi.nl). The gridded SSTs datasets are from the NOAA Extended Reconstructed SST V3b (Smith et al., 2008).

3. Results and Discussion

3.1 Reconstruction of precipitation

The Pearson's correlation coefficients between the tree-ring width/$\delta^{18}O$ and the local precipitation record were the strongest from the previous August to current July. The precipitation (rainfall and snow) from the late growing season to next summer were stored and mixed in soil, which were uptook by trees through roots in next growing season. Therefore information of precipitation $\delta^{18}O$ from the previous August

to current July was recorded by the tree-ring $\delta^{18}O$ in this study. The individual correlations of the previous August to current July precipitation (hereafter, P87) were 0.67 for the ring widths and -0.54 (p<0.0001; n=49) for $\delta^{18}O$. When the series were combined using a simple multiple regression (the ring width index and $\delta^{18}O$ as independent variables, P87 as dependent variable) the multiple correlation coefficient increased to 0.72 (p<0.0001, n=49). Thus, the reconstruction explains 51.9% (50% after adjusting for the loss due to the degrees of freedom) of the variance in the instrumental era P87 (Figure 2a). The available meteorological data are too short for split-period verification, but jack-knife and bootstrap (Efron 1979) verifications indicated that the reconstruction is stable and reliable (Table 1). Because the precipitation in the field area is dominated by the EASM, the reconstructed record likely represents a very large portion of the EASM area. This assumption can be demonstrated by calculating the spatial correlation between the reconstructed P87 and the concurrent CRU TS3 precipitation gridded datasets over the instrument period of 1955-2003 (Figure 1b). Significant correlations (p<0.05) cover a very large area (approximately 30°-45° N, 105°-120° E), including NC, the Loess Plateau and part of the Gobi Desert. These areas are arid or semi-arid areas where moisture is scarce and where any anthropogenically induced changes in the precipitation regime will have serious consequences.

To determine the long-term reliability of the reconstruction in the absence of long-term local precipitation records, we compared the reconstructed precipitation

with several hydroclimate series of NC (Figure2). This reconstruction was significantly correlated with the Dryness/Wetness Index (DWI) that was extracted from historical documents from NC (Shen et al., 2008), the precipitation of Helan Mountian from January to July (Liu et al., 2005) and the annual precipitation of eastern China (east of 105° E) (Wang et al., 2002). Figure 2b-2e expresses the common characteristics of precipitation variability in the EASM area. For example, a drought event from the 1920s to the early 1930s occurred over a large area of NC, which is considered to be one of the most severe droughts that has occurred within the last 500 years (Liang et al., 2006; Kang et al., 2002; Yang et al., 2014a). In addition, a decrease in the amount of precipitation that was detected during the last half of the century in several of the time series (shown in Figure 2) implies that the hydroclimate of NC becomes severe. The drought events occurring in the late 1920s to early 1930s and drought trend in the recent 50 years are clearly demonstrated in many studies (Chen et al., 2012; Fang et al., 2012; Kang et al., 2012, 2013; Liu et al., 2010, 2013; Yang et al., 2014b). Eastern China (Figure 2e) contains part of the lower reaches of the Yangtze River (Wang et al., 2002); therefore, the precipitation only decreased slightly during the last half of the century, as shown in Figure 2e.

Because our reconstruction records capture the annual variability and the observed decrease in precipitation over the instrumental period (Figure 2a) and are significantly correlated with the available evidence of long-term changes in the moisture regime of the broad region, we suggest that it likely provides a reasonable

estimate of the long-term variability of precipitation over NC. Because summer precipitation accounts for 80% of the annual precipitation in the observed record from the Yuanping Meteorological Station, we concluded that our reconstruction of P87 could be regarded as an indicator of the EASM strength.

3.2 Relationship between the reconstructed precipitation and the Indian precipitation

3.2.1 The teleconnection

The spatial correlation of Figure 1b, which represents a portion of the surroundings, indicates a positive correlation with a large area of the Indian subcontinent. A 21-year moving correlation between our reconstructed records and the observed Indian precipitation indicated a persistent, positive correlation during the overlapping period (Figure 3a). The interannual correlation between the time series of our reconstructed precipitation records and the observed Indian precipitation is r=0.32 (p< 0.001, n=132). Both of these records indicated that the highest precipitation occurred in 1956 (Figure 3b). The instrument-based precipitation measurements obtained by the Yuanping Meteorological Station confirmed a teleconnection with the IM precipitation during the overlapping period (r=0.47, p<0.001, n=49), as shown in Figure S3a. The magnitude of precipitation over NC and India are very different. On the Indian subcontinent, a large amount of water vapour is present due to high

amounts of evaporation over the tropical Indian Ocean (Clemens et al., 1991).

Given the differences in the source regions and amounts of precipitation in NC and on the Indian subcontinent, the significant correlations between the Indian precipitation and our reconstructed records (Figure 1b and Figure 3) strongly suggest that a teleconnection linked with large-scale dynamical controls is present.

3.2.2 The potential role of the ENSO in the teleconnection

Increasing evidence indicates that the ENSO may be a very important factor that influences the amount of precipitation that occurs in India and NC (Annamalai et al., 2007; Ashok et al., 2004; Krishnamurthy and Kirtman, 2003; Li et al., 2011a; Wu and Wang, 2002; Wu et al., 2003). Hu et al. (2005) observed that the ENSO-related Indian precipitation is significantly and positively correlated with the amounts of precipitation over NC at an interannual time scale. The two wave-type teleconnection patterns from low latitudes to high latitudes, one is over the East Asian continent and the other is over the western Pacific Ocean, were proposed to explain the effects of the ENSO on the link between precipitation in NC and India (Hu et al., 2005). However, Feng and Hu (2004) proposed that the ISM plays a very important role in the connection between the ENSO and precipitation in NC. Thus, the ENSO does not directly influence precipitation in NC (Feng and Hu, 2004).

The ENSO is the major forcing factor for interannual (or high-frequency) climate variability and is characterised by a 2–7-year cycle (Kumar et al., 1999; Newman et

al., 2011). To determine if any ENSO effects exist, a 2-7 year bandpass Fast Fourier Transform (FFT) filter was used to remove the low-frequency trends from the reconstructed precipitation records of NC and the Indian precipitation records (All Indian Precipitation). The correlation was significant (r=0.29, n=132 and p<0.001) during the overlapping period of 1872-2003 for high-frequency signals (Figure 4a). In addition, the observed local precipitation was well correlated with the Indian precipitation during the instrumental period (Figure S3b). El Niño/La Niña events result in warming/cooling of the sea surface temperature (SSTs) in the tropical eastern Pacific, which alters the SSTs in the western Pacific and Indian Ocean due to Walker circulation (Chowdary et al., 2012). The changing SSTs influence the land-sea thermal contrast and affect the amount of precipitation (Wu et al., 2012a; Zhou et al., 2011). The most significantly correlated fields between our reconstructed precipitation and the Indian precipitation records and the SSTs between 1880 and 2003 are shown in Figures 4b and 4c, respectively. The reconstructed precipitation was only slightly significantly correlated with the SSTs over the equatorial Central Pacific during the summer (June-July-August). However, the Indian precipitation was significantly correlated with the SSTs over a larger area of the equatorial central to eastern Pacific during the previous winter (December-January-February). When El Nino reaches its mature stage during the winter, the equatorial central to eastern Pacific warming influences the SSTs in the tropical Indian Ocean and acts as a discharging capacitor that decreases the Indian precipitation during the monsoon season (Kumar et al., 1999;

Xie et al., 2009; Xie et al., 2010). This explanation is illustrated in Figure 4c. During the summer, the SSTs in the subtropical Northwest Pacific are indirectly influenced by the ENSO, which is mediated by the SSTs of the Indian Ocean (Xie et al., 2010). It is known that ENSO reaches its mature phase in the winer; therefore Figure 4b does not show a significant correlation in summer.

To verify that the ENSO has an indirect influence on precipitation in NC by mediating the ISM, a 21-year sliding-window correlation between our reconstructed records and the Indian precipitation records was compared with a 21-year moving average of the Nino3 SSTs anomalies shown in Figure 5a. The sliding-window correlation series (between our reconstruction and the Indian precipitation) and the Nino 3 series shown in Figure 5a are not correlated; suggesting that the ENSO does not regulate the link between the precipitationin NC and the ISM region. To analyse the interactions between the ENSO, Indian precipitation, and NC precipitation, we determined whether the Indian precipitation mediated the relationship between NC precipitation and the ENSO, which is shown in Figure 5b. The sliding-window correlation series (between our reconstruction and the Nino 3) and the Indian precipitation series were significantly correlated (r=-0.58, n=112, and p<0.001). During the two sub-periods of 1882-1937 and 1938-1993, the correlations (-0.66 and -0.76, respectively) were very significant and stable. For the instrumental observations, the correlation between the Nino 3 SSTs anomalies and the Indian precipitation was more significant (p<0.05) than that between the observed

precipitation and the Nino 3 SSTs anomalies (p=0.29) (Figure S3b). In addition, an 850 hpa wind field indicates that some of the water vapour in the ISM area is propagated eastward to the Bay of Bengal and northeastward to our study area (Figure S4a). Therefore, the covariation of our reconstruction and the Indian precipitation at the interannual time scale in Figure 4a may be caused by the partial water vapour in NC that originated from the ISM area. These results demonstrate that the mechanism that links the precipitation in NC with the Indian water vapour persists over long periods, as proposed by Wu et al. (2012a) that a branch of ISM water vapor is transported northeastward to sustain precipitation over the EASM area. However, uncertainty still exists in our conclusion, which should be supported by more evidences based on modeling efforts and reasonable mechanism in the future.

Interestingly, during the periods of 1895-1899 and 1994-2003, the reconstructed precipitation and the observed Indian precipitation appeared to be in anti-phase (dashed boxes in Figure 4a). Possible reasons may be minimum solar irradiance of 1890s and weaking relationship between the ENSO and ISM (Kumar et al., 1999; Lean, 2000).

3.2.3 The teleconnection for low-frequency signals

The relationships between reconstruction and the Indian precipitation were examined using a 22-year FFT low-pass filter (Figure 6 and Table 2). The correlation between the series was high (r=0.62, n=120), and we used a coral-based ISM proxy

reconstruction to verify and extend the results (Gong and Luterbacher, 2008) (Figure 6). The two records show some degree of coherence, and the correlation has been statistically significant (r=0.38, n=241) since 1779. Althought the degree of freedom is reduced dut to low-pass filter, the long-term trend between the reconstruction and observed (or proxied) Indian precipitation still similar.

The North Atlantic Oscillation (NAO) is one of the most important zonal circulations in middle latitude. We attempt to check whether above the long-term similar trend is affected by NAO. An analysis of the atmospheric circulation fields showed that the NAO index obtained from the National Centres for Environmental Prediction (http://www.ncep.noaa.gov/) was significantly and negatively (r<-0.3, p<0.05) correlated with the instrument-based precipitation over NC and the Indian subcontinent from 1949 to 2006 (Figure S5a). In addition, meteorologists reported that the NAO had a negative effect on precipitation in the EASM and ISM regions (Goswami et al., 2006; Linderholm et al., 2011; Sung et al., 2006; Wu et al., 2012b).

The instrument-based NAO index (Jones et al., 2001) and reconstructed NAO index (Luterbacher et al., 2001) were compared with our reconstructed precipitation and ISM indices at interdecadal time scales (Figure 6). To facilitate this comparison, the five time series were standardised using a Z-score (Runyon et al., 1994). Similar variations are represented in Figure 6. The correlations among the data were high, except for the correlation between the ISM proxy and the instrument-based NAO (Table 2). This result implied that the precipitation in NC and in the ISM region was

related with the NAO at low frequencies over the past 225 years. In addition, the instrumental data showed the same trend (Figure S3c). This result suggested that the NAO could play an important role in linking the precipitation in NC and in the ISM regions. The simplest explanation is that the circulation pattern established with the NAO affects the EASM and ISM. However, more details are still unclear. Additional studies are needed to understand the mechanisms of this interdecadal linkage.

4. Conclusions

In this paper, we used the tree-ring widths of *Pinus tabulaeformis* and the $\delta^{18}O$ contents of *Larix principis-rupprechtii* from sites near Shanxi Province, China, to reconstruct annual precipitation variations for the period from 1779 to 2003. The reconstruction represents the long-term precipitation variability in the EASM over NC. A teleconnection between the precipitation in NC and in the ISM region was detected at the interannual and interdecadal time scales and persisted over the last 225 years. One likely cause of interannual linkage is the transport of Indian Ocean water vapour eastward and northeastward to our study area. The slight correlation between the ENSO and precipitation in NC does not indicate direct causality. Most likely, the ENSO signals in the Indian precipitation were inherited by the precipitation in NC. At the interdecadal time scale, the precipitation in NC and in the ISM region coincided with the NAO variability.

Acknowledgments

We gratefully acknowledge the editor and the anonymous reviewers for improving the quality of the manuscript. This study was financially supported by NSFC (Nos. 41201046 and 40890051), KZZD-EW-04-01, SKLLQG and the West Doctoral Foundation of CAS. This is Sino-Swedish Tree-ring Research Centre (SISTRR) contribution No. 21.

References

Annamalai, H., Hamilton, K. and Sperber, K.R., 2007. The South Asian summer monsoon and its relationship with ENSO in the IPCC AR4 simulations. Journal of Climate, 20(6), 1071-1092.

Ashok, K., Guan, Z., Saji, N. and Yamagata, T., 2004. Individual and combined influences of ENSO and the Indian Ocean dipole on the Indian summer monsoon. Journal of Climate, 17(16), 3141-3155.

Bao, G, Liu, Y and Linderholm, H W., 2012. April–September mean maximum temperature inferred from Hailar pine (Pinus sylvestris var. mongolica) tree rings in the Hulunbuir region, Inner Mongolia, back to 1868 AD. Palaeogeography, Palaeoclimatology, Palaeoecology, 313, 162-172.

Chen, F. et al., 2012. Tree-ring-based reconstruction of precipitation in the Changling Mountains, China, since AD 1691. International journal of biometeorology, 56(4), 765-774.

Chowdary, J. S. et al., 2012. Interdecadal Variations in ENSO Teleconnection to the Indo-Western Pacific for 1870-2007. Journal of Climate, 25(5), 1722-1744.

Clemens, S. et al., 1991. Forcing mechanisms of the Indian Ocean monsoon. Nature, 353(6346), 720-725.

Crowley, T.J. 2000. Causes of climate change over the past 1000 years. Science, 289(5477), 270.

D'Arrigo, R., Wilson, R. and Jacoby, G., 2006. On the long-term context for late twentieth century warming. Journal of Geophysical Research, 111, D03103.

Efron, B. 1979. Bootstrap methods: another look at the jackknife. The annals of Statistics, 7, 1-26.

Etheridge, D., Steele, L.P., Francey, R. and Langenfelds, R., 1998. Atmospheric methane between 1000 AD and present: Evidence of anthropogenic emissions and climatic variability. Journal of Geophysical Research, 103(D13), 15979-15,993.

Fang, K. et al., 2009. Variation of radial growth patterns in trees along three altitudinal transects in

north central China, IAWA journal, 30(4), 443-457.

Fang, K. et al., 2012. Tree-ring based reconstruction of drought variability (1615–2009) in the Kongtong Mountain area, northern China. Global and Planetary Change, 80, 190-197.

Feng, S. and Hu, Q., 2004. Variations in the Teleconnection of ENSO and Summer Rainfall in Northern China: A Role of the Indian Summer Monsoon. Journal of Climate, 17(24), 4871-4881.

Frank, D.C. et al., 2010. Ensemble reconstruction constraints on the global carbon cycle sensitivity to climate. Nature, 463(7280), 527-530.

Gong, D.Y. and Luterbacher, J., 2008. Variability of the low-level cross-equatorial jet of the western Indian Ocean since 1660 as derived from coral proxies. Geophysical Research Letters, 35, L01705.

Goswami, B.N., Madhusoodanan, M., Neema, C. and Sengupta, D., 2006. A physical mechanism for North Atlantic SST influence on the Indian summer monsoon. Geophysical Research Letters, 33(2).

Hu, Z., Wu, R., Kinter, J.L. and Yang, S., 2005. Connection of summer rainfall variations in South and East Asia: role of El Niño–southern oscillation. International journal of climatology, 25(9), 1279-1289.

Huang, J. and Wang, S., 2007. Instability of the teleconnection of summer rainfalls between North China and India. Journal of Tropical Meteorology, 13(1).

Jones, P., Osborn, T. and Briffa, K., 2001. The evolution of climate over the last millennium. Science, 292(5517), 662-667.

Kang, S, Yang, B, and Qin, C.,2012. Recent tree-growth reduction in north central China as a combined result of a weakened monsoon and atmospheric oscillations. Climatic change, 115(3-4), 519-536.

Kang, S. et al.,2013. Extreme drought events in the years 1877–1878, and 1928, in the southeast Qilian Mountains and the air–sea coupling system. Quaternary International, 283, 85-92.

Kang, X., Cheng, G. and Ersi K., 2002. Runoff from mountain outlet in the Heihe region for the past one thousand years by reconstructing tree-rings. Science in China (Series D), 32(8),675-685.

Krishnamurthy, V. and Kirtman, B.P., 2003. Variability of the Indian Ocean: Relation to monsoon and ENSO. Quarterly Journal of the Royal Meteorological Society, 129(590), 1623-1646.

Kumar, K.K., Rajagopalan, B. and Cane, M.A., 1999. On the weakening relationship between the Indian monsoon and ENSO. Science, 284(5423), 2156-2159.

Lean, J., 2000. Evolution of the Sun's spectral irradiance since the Maunder Minimum. Geophysical Research Letters, 27(16), 2425-2428.

Li, J., Chen, F., Cook, E.R., Gou, X. and Zhang, Y., 2007. Drought reconstruction for north central China from tree rings: the value of the Palmer drought severity index. International journal of climatology, 27(7), 903-909.

Li, Q. et al., 2006. Reconstruction of annula precipitation since 1686 A.D. freom Ningwu region, Shanxi Province. Quaternary Sciences, 26(6), 999-1006.

Li, Q., Nakatsuka, T., Kawamura, K., Liu, Y. and Song, H., 2011a. Hydroclimate variability in the North China Plain and its link with El Niño‐Southern Oscillation since 1784 AD: Insights from tree‐ring cellulose $\delta^{18}O$. Journal of Geophysical Research: Atmospheres (1984‐2012),

116(D22).

Li, Q., Nakatsuka, T., Kawamura, K., Liu, Y. and Song, H., 2011b. Regional hydroclimate and precipitation $\delta^{18}O$ revealed in tree-ring cellulose $\delta^{18}O$ from different tree species in semi-arid Northern China. Chemical Geology, 282(1), 19-28.

Liang, E. et al., 2006. The 1920s drought recorded by tree rings and historical documents in the semi-arid and arid areas of northern China. Climatic Change, 79(3-4), 403-432.

Linderholm, H.W. et al., 2011. Interannual teleconnections between the summer North Atlantic Oscillation and the East Asian summer monsoon. Journal of Geophysical Research: Atmospheres (1984–2012), 116(D13).

Liu, Y. et al., 2005. Seasonal precipitation in the south-central Helan Mountain region, China, reconstructed from tree-ring width for the past 224 years. Canadian Journal of Forest Research, 35(10), 2403-2412.

Liu, Y. and Ding, Y., 2008. Analysis and numerical simulations of the teleconnection between Indian summer monsoon and precipitation in North China. Acta Meteorologica Sinica, 22(4).

Liu, Y., Tian, H., Song, H. and Liang, J., 2010. Tree ring precipitation reconstruction in the Chifeng-Weichang region, China, and East Asian summer monsoon variation since AD 1777. J. Geophys. Res, 115, D06103.

Liu, Y., et al., 2013. Annual precipitation variability inferred from tree-ring width chronologies in the Changling-Shoulu region, China, during AD 1853-2007, Dendrochronologia, 31, 290–296.

Luterbacher, J. et al., 2001. Extending North Atlantic oscillation reconstructions back to 1500. Atmospheric Science Letters, 2(1‐4), 114-124.

Ma, L. et al.,2015. Determining changes in the average minimum winter temperature of Horqin Sandy Land using tree ring records. Theoretical and Applied Climatology, 1-8.

Mann, M.E. et al., 2008. Proxy-based reconstructions of hemispheric and global surface temperature variations over the past two millennia. Proceedings of the National Academy of Sciences, 105(36), 13252.

McCarroll, D. et al.,2003. Multiproxy dendroclimatology: a pilot study in northern Finland. The Holocene, 13(6),829-838.

Newman, M., Shin, S.I. and Alexander, M.A., 2011. Natural variation in ENSO flavors. Geophysical Research Letters, 38(14).

Runyon, R.P., Haber, A. and Coleman, K.A., 1994. Behavioral statistics: The core. McGraw-Hill.

Shen, C., Wang, W.C., Hao, Z. and Gong, W., 2008. Characteristics of anomalous precipitation events over eastern China during the past five centuries. Climate Dynamics, 31(4), 463-476.

Smith, T.M., Reynolds, R.W., Peterson, T.C. and Lawrimore, J., 2008. Improvements to NOAA's Historical Merged Land–Ocean Surface Temperature Analysis (1880–2006). Journal of Climate, 21(10), 2283-2296.

Solanki, S.K., Usoskin, I.G., Kromer, B., Schüssler, M. and Beer, J., 2004. Unusual activity of the Sun during recent decades compared to the previous 11,000 years. Nature, 431(7012), 1084-1087.

Sung, M.K. et al., 2006. A possible impact of the North Atlantic Oscillation on the east Asian summer monsoon precipitation. Geophysical Research Letters, 33(21).

Wang, B., Clemens, S.C. and Liu, P., 2003. Contrasting the Indian and East Asian monsoons: implications on geologic timescales. Marine Geology, 201(1-3), 5-21.

Wang, S., Cai, J., Zhu, J. and Gong, D., 2002. The interdecadal variations of annual precipitation in China during 1880's-1990's. Acta Meteorologica Sinica, 60(5), 637-640.

Wigley, T. M. L., Briffa, K.R., and Jones, P. D., 1984. On the average value of correlated time series, with applications in dendroclimatology and hydrometeorology. Journal of climate and Applied Meteorology, 23(2), 201-213.

Wu, G. et al., 2012a. Thermal Controls on the Asian Summer Monsoon. Scientific Reports, 2(404), 1-7.

Wu, R. and Wang, B., 2002. A Contrast of the East Asian Summer Monsoon–ENSO Relationship between 1962–77 and 1978–93. Journal of Climate, 15(22), 3266-3279.

Wu, R., Zeng-Zhen Hu, R. and Kirtman, B.P., 2003. Evolution of ENSO-related rainfall anomalies in East Asia. Journal of Climate, 16(22), 3742-3758.

Wu, Z., Li, J., Jiang, Z., He, J. and Zhu, X., 2012b. Possible effects of the North Atlantic Oscillation on the strengthening relationship between the East Asian summer monsoon and ENSO. International journal of climatology, 32(5), 794-800.

Xie, S.-P. et al., 2010. Decadal Shift in El Niño Influences on Indo–Western Pacific and East Asian Climate in the 1970s. Journal of Climate, 23(12), 3352-3368.

Xie, S.-P. et al., 2009. Indian Ocean Capacitor Effect on Indo–Western Pacific Climate during the Summer following El Niño. Journal of Climate, 22(3), 730-747.

Yang B., et al.,2014a. Drought variability at the northern fringe of the Asian summer monsoon region over the past millennia. Climate dynamics, 43(3-4), 845-859.

Yang, B. et al., 2014b. A 3,500-year tree-ring record of annual precipitation on the northeastern Tibetan Plateau. Proceedings of the National Academy of Sciences, 111(8), 2903-2908.

Yi, L. et al., 2006. Summer temperature variations since 1676 AD in Luya Mountain, Shanxi Province of China, inferred from tree rings. J. Glaciol. Geocryol, 28,330-336.

Yi, L. et al., 2012. Reconstructions of annual summer precipitation and temperature in north-central China since 1470 AD based on drought/flood index and tree-ring records. Climatic Change, 110(1-2), 469-498.

Zhang, R., 1999. The role of Indian summer monsoon water vapor transportation on the summer rainfall anomalies in the northern part of China during the El Nino mature phase. Plateau Meteor, 18(4), 567-574.

Zhou, M., Tian, F., Lall, U. and Hu, H., 2011. Insights from a joint analysis of Indian and Chinese monsoon rainfall data. Hydrology and Earth System Sciences Discussions, 8, 3167-3187.

Figure captions

Figure 1

Map showing the locations of the sampling sites (triangles) and the nearest meteorological station of Yuanping (circle) (a), and the spatial correlation pattern between the reconstructed precipitation with the CRU TS3 precipitation gridded datasets ($p < 0.1$) (b).

Figure 2

Comparison between the reconstructed and observed precipitation variations during the period of 1955-2003 (a): the annual and decadal (bold lines) series of the reconstructed precipitation (b), the DWI (Shen et al., 2008) over NC (c), the January to July precipitation at Mt. Helan (Liu et al., 2005) (d) and the annual precipitation in eastern China (Wang et al., 2002) (e). The increasing aridification of the last half-century and the 1920s drought are also shown.

Figure 3

Reconstructed precipitation in NC based on the tree-ring widths and $\delta^{18}O$, and the observed "All Indian" (IM) precipitation; the bold lines are the 22-year FFT low-pass filter data (b). The 21-year moving correlation coefficient (C.C) is shown (a).

Figure 4

Time series of the 2-7 year bandpass FFT filter between the reconstructed EAM precipitation (left axes) and the observed Indian precipitation (IM, right axes) (a). The dashed boxes show the anti-phase periods. (b) and (c) are the spatial correlation patterns between the reconstruction/ Indian precipitation and CRU TS3 gridded SSTs during their most significant season from 1880 to 2003 ($p<0.1$).

Figure 5

The 21-year sliding-window correlation (purple line) between the reconstruction and Indian precipitation, comparing with the 21-year moving average of the Nino 3 SST anomalies (a); and the 21-year sliding-window correlation (red line) between the reconstruction and the Nino 3 SST anomalies, comparing with the 21-year moving average of the IM precipitation (b).

Figure 6

Comparisons among the reconstruction, observed Indian precipitation, IM proxy (Gong and Luterbacher 2008), observed NAO and reconstructed NAO (Luterbacher et al., 2002) from 1779 to 2003. All of the data are processed by a 22-year low-pass FFT filter and are standardised by a Z-score. Note that the axe of the NAO is reversed.

Fig. 1

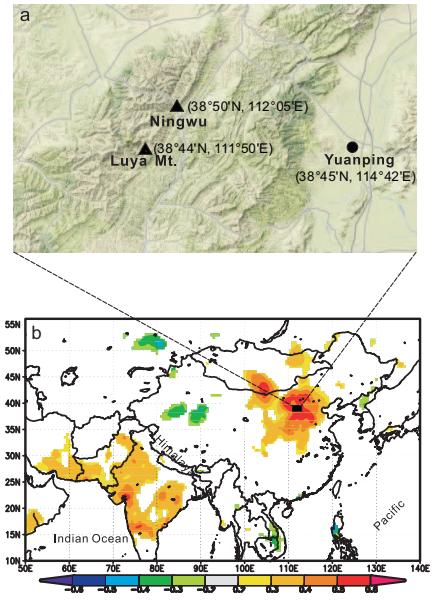

Fig. 2

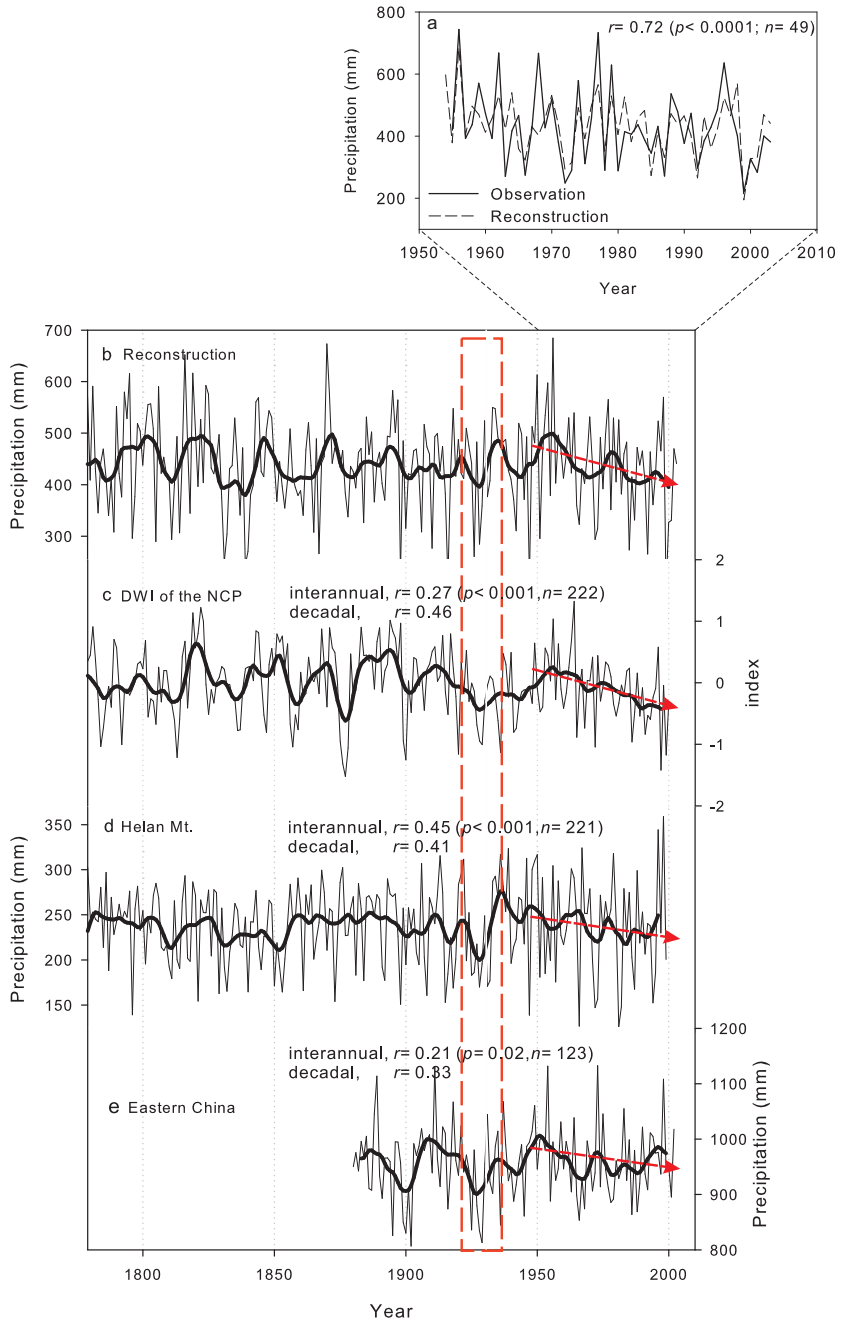

Fig. 3

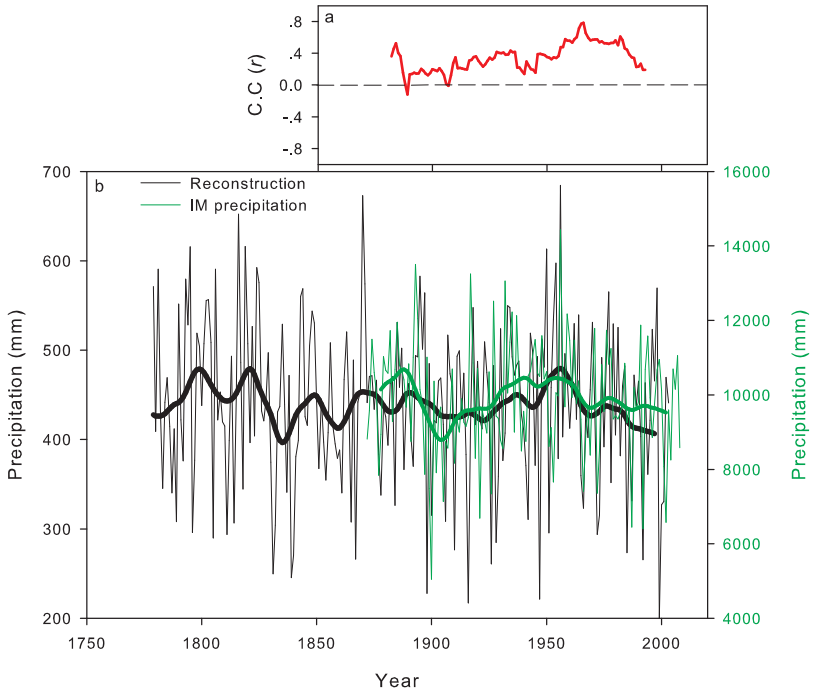

Fig. 4

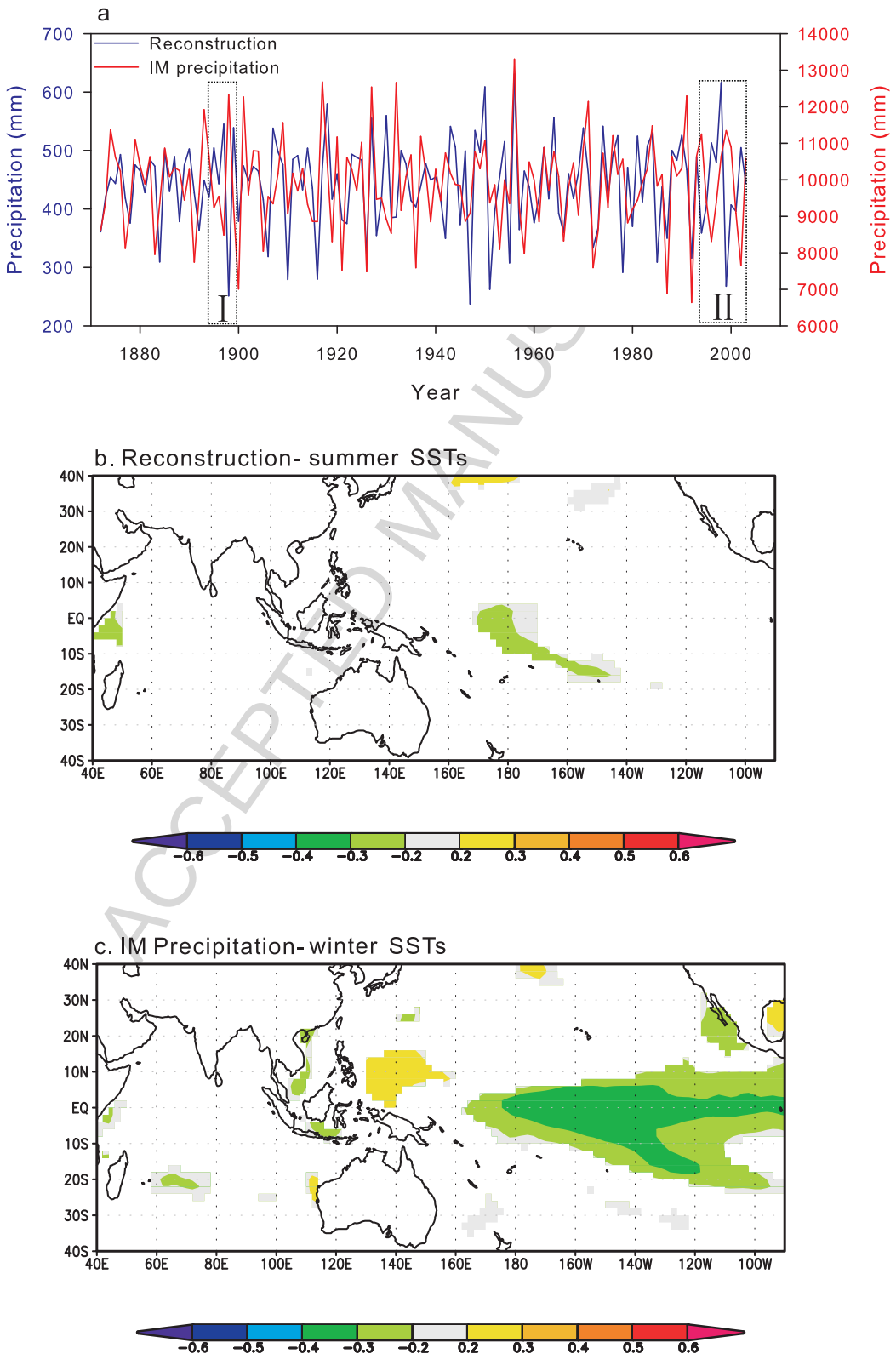

Fig. 5

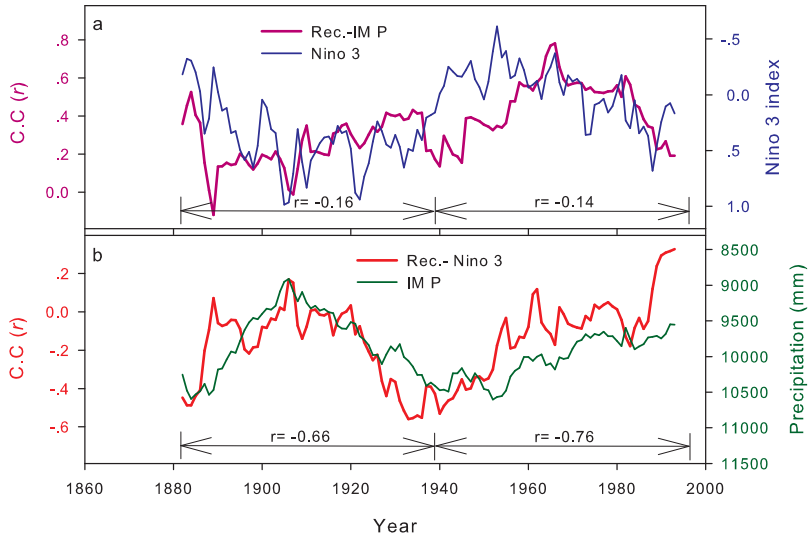

Fig. 6

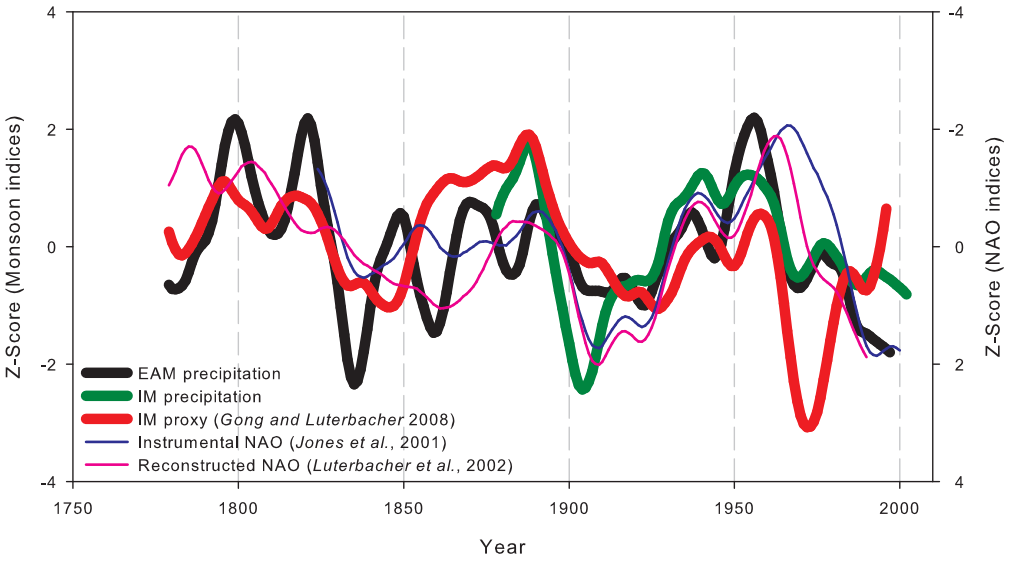

Table 1

Verification statistics of the jack-knife and bootstrap methods for the P87 reconstruction using multiple regression

Statistical items	Jack-knife Mean (range)	Bootstrap (50 iterations) Mean (range)
r	0.72(0.67-0.76)	0.72(0.39-0.85)
R^2	0.52(0.45-0.58)	0.52(0.15-0.73)
R^2_{adj}	0.51(0.44-0.57)	0.51(0.13-0.72)
Standard error of estimate	88.00(79.76-88.96)	87.48(60.55-107.42)
F	50.02(38.20-64.33)	52.26(8.32-124.20)
p	0.0001(0.0001-0.0001)	0.0001(0.0001-0.006)
Durbin-Watson	2.39(2.18-2.54)	2.36(2.11-2.54)

Table 2

Correlation coefficients between the time series (after 22-year low-pass filter) in Figure 6; the number inside the parentheses indicates the *n* of the correlation analysis; all have a $p < 0.001$, except for the correlation coefficient of 0.05

	EASM precipitation	IM precipitation	IM proxy	Instrumental NAO
IM precipitation	0.62(120)			
IM proxy	0.38(218)	0.42(119)		
Instrumental NAO	-0.57(174)	-0.60(123)	0.05(173)	
Reconstructed NAO	-0.52(212)	-0.71(113)	-0.25(212)	0.87(167)

Highlights

High explained variance (51.9%) of the precipitation reconstruction; Detection of a persistent teleconnection between two Asian sub-monsoon systems; The NAO may play a role in such a teleconnection.